JOURNAL OF CATALYSIS 5, 44–54 (1966)

Combined Effect of Volume Change and Internal Heat and Mass Transfer on Gas-Phase Reactions in Porous Catalysts

VERN W. WEEKMAN, JR.

From the Socony Mobil Oil Co., Inc., Research Department, Paulsboro, New Jersey

Received April 19, 1965

The effect of stoichiometry on nonisothermal gaseous bulk-phase reactions in porous catalyst particles has been treated. The results show that for exothermic reactions volume changes during reaction give effectiveness factors which may differ greatly from those predicted by constant volume theory. Endothermic reactions are relatively insensitive to reaction stoichiometry. The triple solutions noted by Weisz and Hicks are also significantly affected by a change in the number of moles during reaction.

Introduction

A most useful tool in analyzing the behavior of chemical reactions within porous catalyst particles has been the concept of the effectiveness factor. In essence this factor represents the ratio of the actual reaction rate to the intrinsic reaction rate if the reactant concentration throughout the catalyst particle is identical to the surface concentration. Damköhler (*1*), Thiele (*2*), and Zeldovich (*3*) were the first to recognize and mathematically formulate the effect of transport phenomena on modifying gas-phase reactions in porous catalyst particles. Wheeler (*4*) and Weisz (*5*, *6*, *8*) have made many contributions in extending this early work. Wei (*18*, *19*) has extended the general analysis of first order systems by Wei and Prater (*20*), to account for intraparticle diffusion.

Prater (*9*) has studied the problem of temperature increases in porous catalysts and has shown that the Damköhler relationship is valid for any geometry or reaction order.

Weisz and Hicks (*10*) have investigated the effect of both heat and mass transfer on nonisothermal reactions in porous catalyst particles. They showed that exothermic reactions can lead to effectiveness factors much greater than 1. Weekman and Gorring (*11*) treated the effect of volume change on isothermal reactions in porous catalyst particles. This work defined the maximum effect of volume change due to reaction in terms of a volume-change modulus and the Thiele modulus. Hawthorne (*12*) studied volume change with nonisothermal reaction, but presented only a limited range of results.

The present work treats volume-change reactions with gaseous bulk diffusion in nonisothermal catalyst particles over a wide range of conditions.

Nomenclature

A	Chemical species, A
a	Constant used in transform, $r = az$
B	Chemical species, B
C_A	Concentration of A (gm moles/cm^3)
C_A^0	Concentration of A at surface temperature (g moles/cm^3)
C_p	Molar heat capacity [(cal/g mole) (°C)]
D_e	Bulk effective diffusivity of A (cm^2/sec)
D_e^0	Bulk effective diffusivity of A at surface temperature (cm^2/sec)
k	Reaction velocity constant (sec^{-1})
k_0	Reaction velocity constant at surface temperature (sec^{-1})
m	Stoichiometric coefficient, A $\rightarrow$ $(1 + m)$B

P Transform $P = dy/dr$
Q Activation energy (cal/g mole)
q_A Molar flux of A [g moles/(cm²) (sec)]
R Gas constant [cal/(g mole) (°K)]
r Dimensionless radius of sphere or depth in flat plate, ξ/ξ_0
T Temperature (°K or °C)
T_0 Surface temperature (°K or °C)
x_A Mole fraction of A
x_A^0 Mole fraction of A external to catalyst particle
y Dimensionless mole fraction, x_A/x_A^0
z Transform variable, $r = az$

Greek Symbols

β Ratio of heat release to heat transport modulus, $D_eC_A\Delta H/\lambda T_0$
β_0 β evaluated at T_0
γ_0 Arrhenius group, Q/RT_0
ΔH Heat of reaction (cal/g mole)
ζ Dimensionless temperature (T/T_0)
η Effectiveness factor, Eqs. (11), (15), (17)
θ Volume-change modulus, $x_A^0 m$
λ Thermal conductivity of catalyst (cal/(sec) (cm) °C)
ξ Radial position in sphere or depth in flat plate (cm)
ξ_0 Radius of sphere or depth of flat plate (cm)
φ_0 Diffusional-kinetic modulus (Thiele), $\xi_0\sqrt{k_0/D_e^0}$
Ω Cross-sectional area (cm²)

Development of Equations

In the derivation of the defining equations it is assumed that surface diffusion, thermal diffusion, adsorption kinetics and equilibria, and external mass transfer resistance are absent. The diffusivity of any inert diluent in the feed is assumed to be the same with respect to both reactant A and product B. Thus a single diffusion coefficient, D_e, is assumed to apply in the catalyst pores.

As derived previously (*11*), the flux of reactant A in any pore, under bulk diffusion conditions, is as follows:

$$q_A = -\frac{D_eC_A(dy/d\xi)}{(1+\theta y)} \qquad (1)$$

The volume-change modulus, $\theta = x_A^0 m$, is composed of an "expansion" factor, m, multiplied by a "dilution factor," x_A^0, which together give a measure of the net "intensity" of the volume-change effect. The factor m is defined by the stoichiometric equation for A reacting to give B as follows:

$$A \rightarrow (1+m)B$$

The ratio of the mole fraction of reactant A at any radial position to the surface mole fraction of A is given by y. For nonisothermal reactions the flux of A becomes (*13*)

$$q_A = -\frac{D_e^0C_A^0\zeta^{1/2}(dy/d\xi)}{(1+\theta y)} \qquad (2)$$

In the above expression it is assumed that ideal bulk diffusion prevails (i.e., $D_e = D_e^0\zeta^{3/2}$, where $\zeta = T/T_0$) and the gases are ideal (i.e., $C_A = C_A^0/\zeta$). For a first order reaction, a simple material balance on a differential catalyst element yields the following expression:

$$d(q_A\Omega)/d\xi = -\Omega C_A^0 ky/\zeta \qquad (3)$$

Assuming an Arrhenius relation, the above equation becomes for spheres

$$\frac{d(\xi^2 q_A)}{d\xi} = -\frac{\xi^2 C_A^0 yk_0 \exp[\gamma_0(\zeta-1)/\zeta]}{\zeta} \qquad (4)$$

Introducing the Thiele modulus, φ_0, and normalizing the radius gives the desired form

$$d\left[\frac{r^2\zeta^{1/2}(dy/dr)}{(1+\theta y)}\right]\Big/ dr = \frac{\varphi_0^2 y \exp[\gamma_0(\zeta-1)/\zeta]}{\zeta} \qquad (5)$$

The dimensionless temperature, ζ, may be related to dimensionless reactant concentration, y, by a Damköhler's relation. Thus for the steady state at any spherical shell, the heat released by reaction must equal the heat being conducted away.

$$q_A(\Delta H) = \lambda T_0(d\zeta/d\xi). \qquad (6)$$

Substitution of Eq. (1) into Eq. (6) gives

$$dy/(1+\theta y) = -d\zeta/\beta \qquad (7)$$

where

$$\beta = D_eC_A\Delta H/\lambda T_0$$

The dimensionless group β will be some function of the dimensionless temperature

ζ, depending upon which catalysts and reactants are used. If the effect of temperature on the heat of reaction and on the catalyst thermal conductivity tend to cancel each other, or if they are negligible, then for bulk diffusion, β becomes

$$\beta = \beta_0 \zeta^{1/2} \tag{8}$$

Substituting Eq. (8) into Eq. (7) and solving with the appropriate boundary conditions ($y = 1, \zeta = 1$), leads to the following relation:

$$\zeta = \left[1 + \frac{\beta_0}{2\theta} \ln \frac{1 + \theta}{1 + \theta y}\right]^2 \tag{9}$$

Substitution of this expression into Eq. (5) followed by differentiation gives the desired form of the equation describing heat and mass transfer within a sphere.

$$\frac{d^2y}{dr^2} - \left[\frac{\theta + (\beta_0/2\zeta^{1/2})}{1 + \theta y}\right]\left(\frac{dy}{dr}\right)^2 + \frac{2}{r}\frac{dy}{dr} = \frac{\varphi_0^2 y(1 + \theta y) \exp\left[\gamma_0(\zeta - 1)/\zeta\right]}{\zeta^{3/2}} \tag{10}$$

The appropriate boundary conditions are

(a) $dy/dr = 0, \quad r = 0$

(b) $y = 1, \quad r = 1$

Knowing the concentration gradient at the surface, one can readily calculate the effectiveness factor

$$\eta = \frac{4\pi\xi_0^2 q_A|_{\xi=\xi_0}}{\frac{4}{3}\pi\xi_0^3 k_0 C_A{}^0} = \frac{3(dy/dr)_{r=1}}{\varphi_0^2(1 + \theta)} \tag{11}$$

The concentration gradient at $r = 1$ is obtained from the numerical solution of Eq. (10) described in a later section.

For isothermal, constant-volume reactions (i.e., $\theta = 0, \beta = 0$), Eq. (10) reduces exactly to that of Thiele (*2*). For isothermal reactions with volume expansion (i.e., $\theta \neq 0$, $\beta = 0$) Eq. (10) reduces exactly to that of Weekman and Gorring (*11*). For nonisothermal reactions without volume expansion (i.e., $\theta = 0$, $\beta \neq 0$), Eq. (10) reduces approximately to that given by Weisz and Hicks (*10*). The difference may be attributed to the fact that the latter authors treated the reactant flux, q_A [Eq. (2)] as independent of temperature. To determine the sensitivity of the analysis to the dependence of β and the reactant flux on temperature, the following cases were analyzed:

1. $\beta = \beta_0 \zeta^{-1/2}$
2. $\beta = \beta_0$
3. $\beta = \beta_0 \zeta^{1/2}$
4. $\beta = \beta_0 \zeta$

Figure 1 compares the above examples with the work of Weisz and Hicks. Appendix I lists the appropriate equations for these cases. The greatest differences are noted at the highest values of η and are of secondary importance for $\beta_0 < 0.4$ and $\gamma_0 < 20$. In fact, Case 3 is very close to the results of Weisz and Hicks. In all the work to follow, the third case, i.e., $\beta = \beta_0 \zeta^{1/2}$, was used because it will be typical of many reacting systems. For high values of β and γ the dependence of β on temperature may have significant effects on η, and caution is advised in these areas.

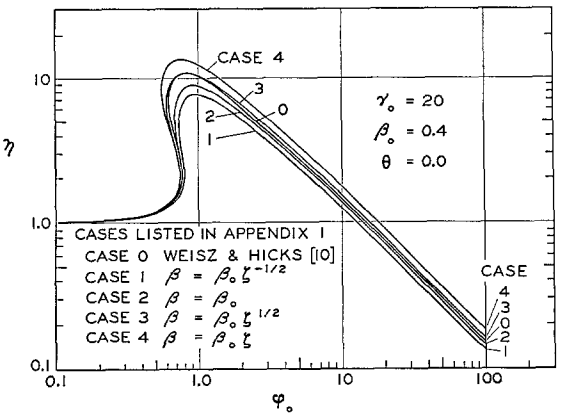

FIG. 1. Effect of temperature on the heat release to heat transport modulus β.

Effect of Volume Change

Solution of Eq. (10) with Eq. (9) for various degrees of volume expansion is plotted on Fig. 2 and reveals the important result that volume change has a *profound effect* on exothermic reactions in porous catalysts. For exothermic reactions volume contraction causes large *increases* in catalyst effectiveness, and volume expansion greatly *reduces* it, relative to the effectiveness of the catalyst obtained from the constant volume solutions at the same diffusional-kinetic modulus, φ_0.

Figure 3 shows that for endothermic reactions volume change has much less effect. This is primarily due to the self-quenching effect of endothermic reactions. Thus, volume contraction (less resistance to diffusion) causes a greater temperature gradient but little change in the average reaction rate. With volume expansion, less reactant can penetrate into the bead, resulting in a reduced temperature gradient. Thus, with both volume expansions and contractions during endothermic reactions, there are compensating effects which result in only small changes in catalyst effectiveness.

Figures 4–12 show the effect of volume expansion for various values of the volume-expansion modulus θ and the dimensionless groups γ_0 and β_0. For exothermic reactions (i.e., $\beta_0 > 0$) the multiple solutions, first noted and explained by Weisz and Hicks (*10*), are also observed with volume-expansion and contraction effects. The present results agree very closely with those obtained for the limited range of parameters investigated by Hawthorne (*12*) for nonisothermal, volume-change reactions. For certain ranges of γ_0 and β_0, volume expansion causes only a single solution to appear, whereas the constant-volume case ($\theta = 0$) gives multiple solutions. Inspection of Figs. 4 and 6 reveals this effect.

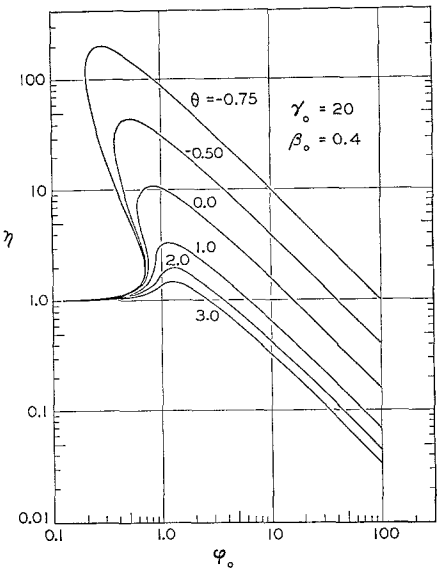

Fig. 2. Effect of volume change on an exothermic reaction in a porous catalyst particle.

Volume contraction can cause a multiple solution to appear where none was observed for no molar change. By contrasting Figs. 6 and 8 one can see that for $\theta = 0$ triple solutions appear when $\gamma_0\beta_0 > 6$ while for $\theta = -0.75$ triple solutions appear for $\gamma_0\beta_0 > 3$.

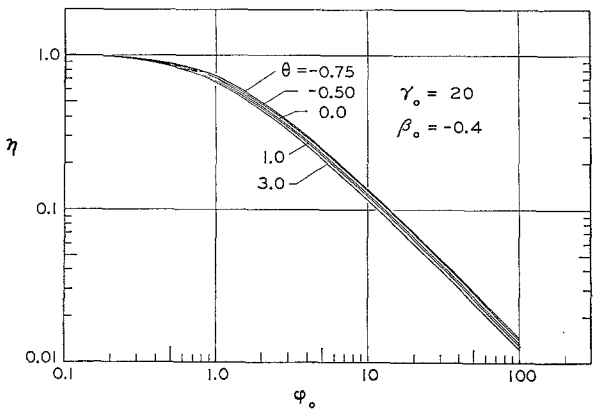

Fig. 3. Effect of volume change on an endothermic reaction in a porous catalyst particle.

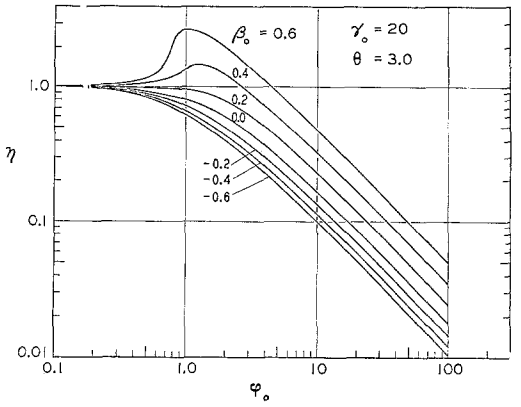

FIG. 4.

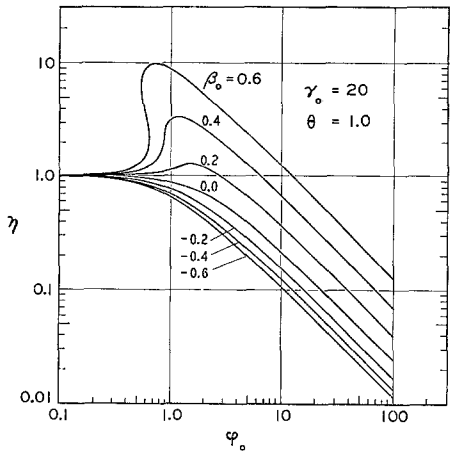

FIG. 5.

FIGS. 4 AND 5. Effectiveness of porous catalyst particles with nonisothermal volume-expansion reactions.

With volume expansion the effectiveness factor for an exothermic reaction may be suppressed so that for all values of reaction modulus φ_0, no effectiveness factors greater than unity are observed. Figure 4 provides an example of this phenomenon.

Thus, volume change can have a profound effect on exothermic reactions in porous catalyst particles operated in the bulk-diffusion region when compared to constant-volume theory for the same diffusional-kinetic modulus. As an example, we may speculate that gas-phase hydrogenation reactions in porous catalysts operating in the bulk diffusion region may exhibit large increases in catalyst effectiveness. The high heats of reaction and substantial volume

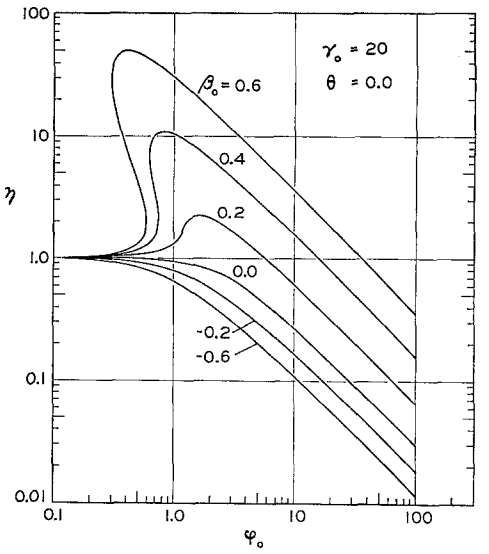

FIG. 6. Effectiveness of porous catalyst particles with constant-volume nonisothermal reactions.

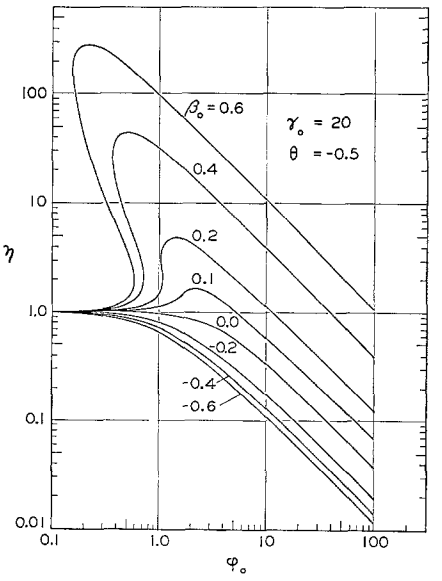

FIG. 7. Effectiveness of porous catalyst particles for nonisothermal volume-contraction reactions.

contraction effects common to hydrogenation reactions all tend to increase the effectiveness above that predicted by isothermal constant-volume theory. The multiple solution effect may be the cause of the instability and sensitivity of hydrogenation reactions in certain operating regions. As pointed out by Weisz and Hicks (*10*), the steady state

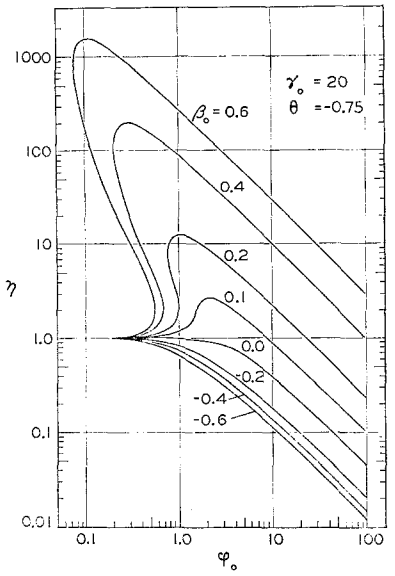

FIG. 8. Effectiveness of porous catalyst particles for nonisothermal volume-contraction reactions.

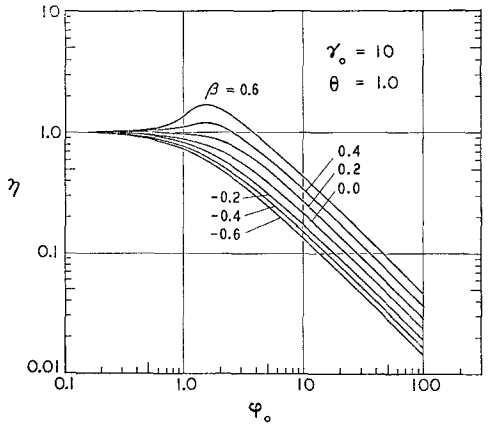

FIG. 9. Effectiveness of porous catalyst particles with nonisothermal volume-expansion reactions.

operating point may depend on the conditions from which the steady state is approached. The present analysis shows that with volume contraction these effects may even be more pronounced, although volume expansion will tend to minimize them.

MAXIMUM TEMPERATURE RISE

The maximum temperature in a catalyst bead will occur when the reactant is exhausted (i.e., $y = 0$). Under these conditions Eq. (9) becomes

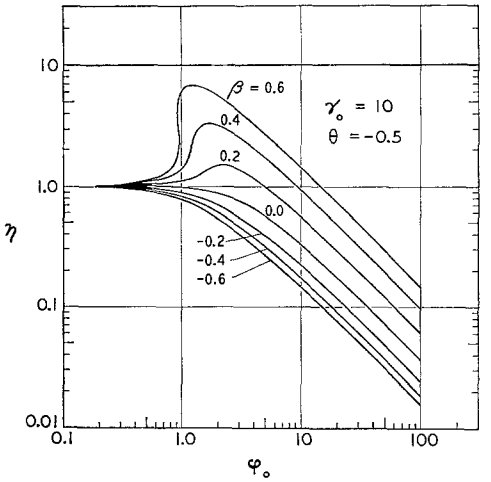

FIG. 10. Effectiveness of porous catalyst particles for nonisothermal volume-contraction reactions.

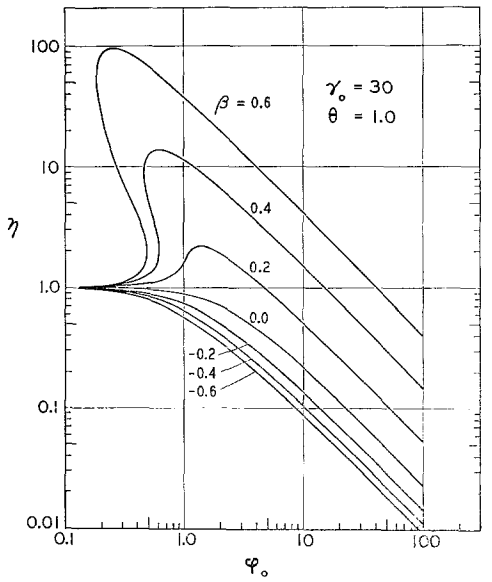

FIG. 11. Effectiveness of porous catalyst particles with nonisothermal volume-expansion reactions.

$$\zeta_{max} = [1 + (\beta_0/2\theta) \ln (1 + \theta)]^2 \quad (12)$$

As the volume-*expansion* effect gets larger and larger, the ratio of maximum internal temperature to surface temperature, ζ_{max}, approaches 1. However, as the volume-*contraction* effect tends toward the maximum, as θ approaches -1, the maximum temperature becomes very large.

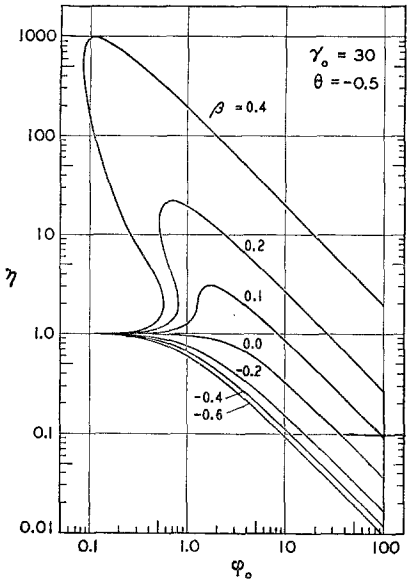

FIG. 12. Effectiveness of porous catalyst particles for nonisothermal volume-contraction reactions.

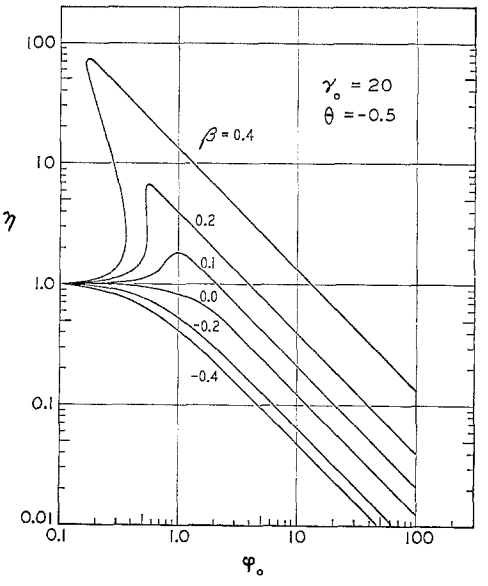

FIG. 14. Flate Plate Solution.

Thus for exothermic reactions, with large volume-*contraction* effects, very large temperature increases are possible. For example, a 4 to 1 contraction with $\beta_0 = 0.5$ could lead to a maximum temperature greater by a factor of 2.1 than the surface temperature.

ASYMPTOTIC SOLUTIONS

With exothermic reactions the reactant concentration approaches zero at small values of φ_0. For example, for $\gamma_0 = 20$, $\beta_0 = 0.6$, and $\theta = -0.75$ the dimensionless reactant concentration was only 10^{-34} at $\varphi_0 = 0.5$. Since the numerical integration methods require a finite concentration to begin a marching solution, calculation of η for higher values of φ_0 is extremely difficult by conventional means. Weisz and Hicks (*10*) employed extrapolation techniques to obtain values of η at values of φ_0 for which virtual reactant exhaustion occurs.

By employing an asymptotic solution, previously developed by Weekman and Gorring (*11*), it was possible to obtain values of η, at arbitrarily large values of φ_0, to a high degree of accuracy. When the center concentration is essentially zero, (i.e., $\varphi_0 > 10$)

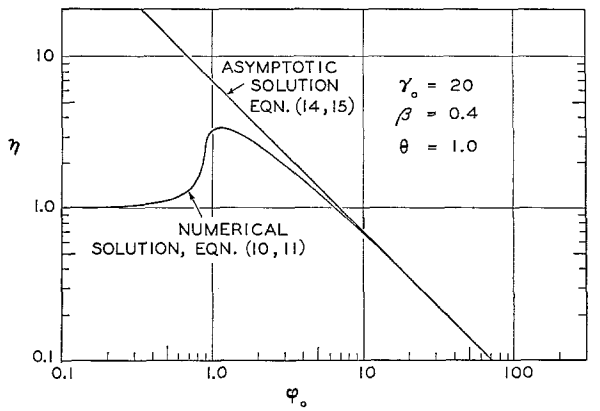

FIG. 13. Comparison of asymptotic and numerical solution.

most of the reaction will be taking place in a small shell at the surface (*14*). This region may be well defined by the flat plate equivalent of Eq. (10) given as Eq. (13)

$$\frac{d^2y}{dr^2} - \left[\frac{\theta + (\beta_0/2\zeta^{1/2})}{1 + \theta y}\right]\left(\frac{dy}{dr}\right)^2 = \frac{\varphi_0^2 y(1 + \theta y)\exp[\gamma_0(\zeta - 1)/\zeta]}{\zeta^{3/2}} \quad (13)$$

On making the transformation $P = dy/dr$, Eq. (13) becomes

$$\frac{dP^2}{dy} - 2\left[\frac{\theta + (\beta_0/2\zeta^{1/2})}{1 + \theta y}\right]P^2 = \frac{2\varphi_0^2 y(1 + \theta y)\exp[\gamma_0(\zeta - 1)/\zeta]}{\zeta^{3/2}} \quad (14)$$

Employing Eq. (9), Eq. (14) was solved by a fourth order Runga-Kutta-Gill integration technique. The appropriate boundary condition is $y = 0$, $P = 0$. The integration proceeds to $y = 1$, and the effectiveness factor is then computed as follows:

$$\eta = 3P_{(y=1)}/[\varphi_0^2(1 + \theta)] \quad (15)$$

Figure 13 shows the convergence of Eq. (10) to the asymptotic solution of Eq. (14). All values of η for high values of φ_0 were determined by this asymptotic solution approach.

Numerical Solution

The split boundary value problem presented by Eq. (10) can be transformed to an initial value problem by the transformation $r = az$. This transformation was suggested by J. Wei of this Laboratory and has also been employed by Weisz and Hicks (*10*). Under this transformation Eq. (10) becomes

$$\frac{d^2y}{dz^2} - \left[\frac{\theta + (\beta_0/2\zeta^{1/2})}{1 + \theta y}\right]\left(\frac{dy}{dz}\right)^2 + \frac{2}{z}\frac{dy}{dz} = \frac{a^2\varphi_0^2 y(1 + \theta y)\exp[\gamma_0(\zeta - 1)/\zeta]}{\zeta^{3/2}} \quad (16)$$

A fourth order Runga-Kutta-Gill integration technique (*15*) was used to solve this initial value problem. Given an assumed value for $a\varphi_0$ and $y(0)$, the integration proceeded to $y = 1$. Using the value of z at $y = 1$ and knowing $r = 1$ at $y = 1$, the value of a and φ_0 could then be calculated. The effectiveness factor under this transformation then becomes

$$\eta = \frac{3(dy/dz)_{r=1}}{a\varphi_0^2(1 + \theta)} \quad (17)$$

By employing Eq. (10) in the form used by Weisz and Hicks (*10*), the present computer program checked their results to 1 part in 10^5 (*16*). On an IBM 7040 computer an entire figure, such as Fig. 5, could be computed in approximately 10–15 min. Typical step sizes ranged from 1/250 to 1/1000 based on the normalized radius r.

The asymptotic solutions were also computed by the same fourth order Runga-Kutta-Gill method and the step size was 1/512 based on the normalized concentration y. In all cases increased step sizes had no effect on the accuracy or stability of the solution.

Interpolations and Extrapolations

Carberry (*17*) reported nonisothermal effectiveness factors in terms of the diffusional-kinetic modulus, and the product $\gamma_0\beta_0$. Inspection of the results of Weisz and Hicks (*10*) reveals that $\gamma_0\beta_0$ parameter is fairly adequate when the diffusional-kinetic modulus φ_0 is not in the triple solution region, and $\beta_0 < 0.2$. From Eqs. (9) and (10) we see that while the product $\gamma_0\beta_0$ appears in the exponential term, β_0 also appears separately. Thus, presenting the calculations based on the product $\gamma_0\beta_0$ has validity only when $\gamma_0\beta_0$ dominates the solution.

Equation (9) reveals that as β_0 approaches zero and becomes negative or as θ gets large, the dimensionless temperature ratio becomes less dependent on β_0 and the $\gamma_0\beta_0$ term will be increasingly important. Conversely, as θ approaches -1, the value of β_0 becomes increasingly important, and, under this condition, characterizing the solution of Eq. (10) by only $\gamma_0\beta_0$ can be expected to give large errors. A study of the numerical solutions of Eq. (10) confirms these observations. Thus Table 1 reveals that for exothermic reactions, characterizing the solution with only the $\gamma_0\beta_0$ parameter leads to large errors for volume-contraction reactions, but gives a reasonable characterization of volume-expansion reactions, provided the value of φ_0 is not in the triple solution region.

Endothermic reactions can be characterized adequately by the single $\gamma_0\beta_0$ parameter.

Thus for all endothermic reactions and for exothermic reactions with volume expansion, the $\gamma_0\beta_0$ parameter can be used for interpolating or extrapolating the present numerical results. This method will be hazardous for values of φ_0 in the triple solution region and for exothermic volume-contraction reactions, and is not recommended under these conditions.

TABLE 1
TEST OF UNIQUE DEPENDENCE OF EFFECTIVENESS FACTOR ON THE PRODUCT $\gamma_0\beta_0$

β_0	γ_0	η at $\varphi_0 = 1$	η at $\varphi_0 = 10$
		$\gamma_0\beta_0 = 2.0$	$\theta = -0.5$
0.2	10	1.1	0.55
0.1	20	1.1	0.58
		$\gamma_0\beta_0 = 6.0$	$\theta = -0.5$
0.6	10	6.0	1.4
0.2	30	19.0	2.6
		$\gamma_0\beta_0 = 12$	$\theta = -0.5$
0.6	20	97	10.5
0.4	30	190	19.2
		$\gamma_0\beta_0 = 6$	$\theta = 1.0$
0.6	10	1.3	0.43
0.2	30	1.6	0.50
		$\gamma_0\beta_0 = 12$	$\theta = 1.0$
0.6	20	8.8	1.2
0.4	30	11.2	1.4
		$\gamma_0\beta_0 = -6.0$	$\theta = -0.5$
−0.6	10	0.77	0.145
−0.2	30	0.76	0.150

An example of using this method to predict effectiveness factors for conditions not explicitly covered by the present numerical work will be instructive. Find the effectiveness of a catalyst particle under the following conditions; $\theta = 3$, $\gamma_0 = 40$, $\beta_0 = 0.1$, $\varphi_0 = 2$. From Fig. 4 ($\theta = 3$, $\gamma_0 = 20$) we can look up the effectiveness factor at $\gamma_0\beta_0 = 4$ from the $\beta_0 = 0.2$ curve (since $\gamma_0\beta_0 = 4$). The value of $\varphi_0 = 2$ is outside the range of possible triple solutions (i.e., $\varphi_0 > 1.2$) so the approximation is valid.

EFFECT OF PARTICLE GEOMETRY

The Aris (*14*) approximation is essentially a shifting of the diffusional-kinetic modulus to give a common curve for all geometries with constant-volume, isothermal reactions. It was shown previously (*11*) that such an approximation was also valid for volume-change reactions. The approximation improves as φ_0 becomes greater, since the reaction tends to occur only near the surface of the particle and thus assumes the shape of flat plate geometry. The "shifted" value of φ_0 to use with the spherical geometry results of this report is as follows:

$$\varphi'_0 = (3V_p/S_x)(k/D_e)^{1/2} \qquad (18)$$

where V_p is the particle volume and S_x is its external surface area.

Thus, to use the results of Figs. 4–12 for other geometries, the following relationships are necessary:

$\varphi'_0 = 3\varphi_0$ for Flat Plates
$\varphi'_0 = 2\varphi_0$ for Cylinders
$\varphi'_0 = \varphi_0$ for Spheres

Figure 14 shows a typical numerical solution for flat plate geometry (Eq. 13) which may be used to test the Aris approximation for nonisothermal volume-change reactions. Table 2 shows that the approximation is very good for exothermic reactions when the value of the diffusional-kinetic modulus is outside the triple solution region. For endothermic reactions the approximation is quite good over the entire range of the diffusional-kinetic modulus.

CONCLUSIONS

It has been shown that volume change has a profound effect on catalyst effectiveness for exothermic reactions. For the same diffusional-kinetic (Thiele) modulus, volume contraction gives large increases in the effectiveness factor of exothermic reactions, whereas volume expansion gives large decreases.

For endothermic reactions the analysis revealed that volume change has much less effect than on exothermic reactions. The self-quenching effect of endothermic reac-

TABLE 2
TEST OF ARIS APPROXIMATION

φ_0	φ'_0	η estimated from Fig. 7	η calculated for Flat Plates
		$\gamma_0 = 20$	
		Exothermic Reactions — Flat Plates	
	$\theta = -0.5$	$\beta = 0.4$	
0.1	0.3	1.03	1.01
0.3	0.9	34.0	(Triple Soln.)
0.6	1.8	19.1	21.5
1.0	3.0	12.1	13.0
3.0	9.0	4.3	4.4
6.0	18.0	2.2	2.2
10.0	30.0	1.3	1.3
30.0	90.0	0.44	0.44
		Endothermic Reactions — Flat Plates	
	$\theta = -0.5$	$\beta = -0.4$	
0.1	0.3	0.94	0.98
0.3	0.9	0.75	0.81
0.6	1.8	0.52	0.59
1.0	3.0	0.37	0.41
3.0	9.0	0.14	0.15
6.0	18.0	0.075	0.076
10.0	30.0	0.046	0.046
30.0	90.0	0.016	0.016

tions is the main reason for this small effect.

For exothermic reactions with accompanying volume contraction, the region of multiple solutions observed by Weisz and Hicks (*10*), will occur at much smaller values of the heat release to heat transport modulus. Thus for certain gaseous catalytic reactions, with high attendant exothermic heat of reaction and volume contraction, the effectiveness of porous pellets may be much greater than predicted from intrinsic rate data or from constant-volume effectiveness factor plots. Consideration of the volume-change effects reveals that multiple solutions tend to disappear or become more pronounced, depending on the degree of volume change.

A technique is presented for extrapolating or interpolating the present results for conditions not given explicitly by the numerical solutions. It is shown that the present nonisothermal volume-change results may be extended to any particle shape, provided the region of triple solutions is avoided.

In summary, when a given exothermic reaction leads to significant volume expansion or contraction, the average reaction rate in a catalyst particle may differ greatly from that predicted by constant-volume theory.

ACKNOWLEDGMENT

The digital computer programming assistance of R. A. Eimer of this Laboratory is gratefully acknowledged.

APPENDIX I

Case 1

$$\beta = \beta_0 \zeta^{-1/2}$$

$$\zeta = \left[1 + \frac{3\beta_0}{2\theta} \ln \frac{1+\theta}{1+\theta y}\right]^{2/3}$$

$$\frac{d^2y}{dr^2} - \left[\frac{\theta + (\beta_0/2\zeta^{3/2})}{1+\theta y}\right]\left(\frac{dy}{dr}\right)^2 + \frac{2}{r}\frac{dy}{dr} = \frac{\varphi_0^2 y(1+\theta y)\exp\left[\gamma_0(\zeta-1)/\zeta\right]}{\zeta^{3/2}}$$

Case 2

$$\beta = \beta_0$$

$$\zeta = 1 + \frac{\beta_0}{\theta} \ln \frac{1+\theta}{1+\theta y}$$

$$\frac{d^2y}{dr^2} - \left[\frac{\theta + (\beta_0/2\zeta)}{1+\theta y}\right]\left(\frac{dy}{dr}\right)^2 + \frac{2}{r}\frac{dy}{dr} = \frac{\varphi_0^2 y(1+\theta y)\exp\left[\gamma_0(\zeta-1)/\zeta\right]}{\zeta^{3/2}}$$

Case 3

$$\beta = \beta_0 \zeta^{1/2}$$

$$\zeta = \left[1 + \frac{\beta_0}{2\theta} \ln \frac{1+\theta}{1+\theta y}\right]^2$$

$$\frac{d^2y}{dr^2} - \left[\frac{\theta + (\beta_0/2\zeta^{1/2})}{1+\theta y}\right]\left(\frac{dy}{dr}\right)^2 + \frac{2}{r}\frac{dy}{dr} = \frac{\varphi_0^2 y(1+\theta y)\exp\left[\gamma_0(\zeta-1)/\zeta\right]}{\zeta^{3/2}}$$

Case 4

$$\beta = \beta_0 \zeta$$

$$\zeta = \left(\frac{1+\theta}{1+\theta y}\right)^{\beta_0/\theta}$$

$$\frac{d^2y}{dr^2} - \left[\frac{\theta + (\beta_0/2)}{1+\theta y}\right]\left(\frac{dy}{dr}\right)^2 + \frac{2}{r}\frac{dy}{dr} = \frac{\varphi_0^2 y(1+\theta y)\exp\left[\gamma_0(\zeta-1)/\zeta\right]}{\zeta^{3/2}}$$

References

1. Damköhler, G., "Der Chemie Ingenieur," Vol. III, p. 430. Akademische Verlagsgesellschaft M.B.H., Leipzig, 1937.
2. Thiele, E. W., *Ind. Eng. Chem.* **31,** 916 (1939).
3. Zeldovich, Y. B., *Acta Physicochem, URSS* **10,** 583 (1939).
4. Wheeler, A., *Advan. Catalysis* **3,** 249–327 (1951).
5. Weisz, P. B., and Prater, C. D., *Advan. Catalysis* **6,** 143–196 (1954).
6. Weisz, P. B., and Swegler, E. W., *J. Phys. Chem.* **59,** 823 (1955).
7. Prater, C. D., and Lago, R. M., *Advan. Catalysis* **8,** 293 (1956).
8. Weisz, P. B., *Chem. Eng. Prog. Symp. Ser.,* (No. 25), **55,** 29 (1959).
9. Prater, C. D., *Chem. Eng. Sci.* **8,** 284 (1958).
10. Weisz, P. B., and Hicks, J. S., *Chem. Eng. Sci.* **17,** 265 (1962).
11. Weekman, V. W., Jr., and Gorring, R. L., *J. Catalysis* **4,** 260 (1965).
12. Hawthorne, R. D., paper presented at AIChE meeting New York, Dec. 2–7, 1961.
13. Hirschfelder, J. O., Curtiss, C. F., and Bird, R. B., "Molecular Theory of Gases and Liquids," p. 516. Wiley, New York, 1964.
14. Aris, R., *Chem. Eng. Sci.* **6,** 262 (1957).
15. Lapidus, L., "Digital Computation for Chemical Engineers," p. 90. McGraw-Hill, New York, 1962.
16. Hicks, J. S., private communication.
17. Carberry, J. J., *AIChE J.* **7,** (No. 2), 350 (1961).
18. Wei, J., *J. Catalysis* **1,** 526 (1962).
19. Wei, J., *J. Catalysis* **1,** 538 (1962).
20. Wei, J., and Prater, C. D., *Advan. Catalysis* **13,** (1962).